Journal of the European Ceramic Society 15 (1995) 675–681

0955-2219/95/$9.50

0955-2219(95)00019-4

Structural Evolution of Non-Crystalline SiC Precursors Prepared from Tetra methoxysilane (TMOS) and Phenol Resin

Hartmut Schneider,[a] Christian Jäger,[b] Alain Mosset,[c] Hidehiko Tanaka[d] & Martin Schmücker[a]

[a]German Aerospace Research Establishment (DLR), Institute for Materials Research, Linder Höhe, D-51140 Köln, Germany
[b]Max-Planck-Institute of Polymer-Research, Ackermannweg 10, D-55128 Mainz, Germany
[c]CEMES-LOE/CNRS, B. P. 4347, F-31055 Toulouse Cedex, France
[d]National Institute for Research in Inorganic Materials (NIRIM), Namiki 1-1, Tsukuba-shi, Japan

(Received 20 June 1994; revised version received 16 August 1994; accepted 26 January 1995)

Abstract

The structural evolution of SiC precursors prepared from tetramethoxysilane (TMOS) and phenol resin by H_2O polymerization and heat-treated between 80 and 1400°C was investigated by X-ray diffractometry (XRD), large-angle X-ray scattering (LAXS), transmission electron microscopy (TEM), and by ^{29}Si and ^{13}C nuclear magnetic resonance spectroscopy (NMR).

After hydrolysis and drying at about 80°C, the samples structurally consist of domains of partially hydrogenated silica and of coexisting phenol resin. Heat-treatments carried out on the predried material yield different stages of structural evolution, though the precursor is non-crystalline throughout the whole temperature field investigated:

— Stage I (≤500°C): gradual temperature-dependent decomposition of phenol resin and simultaneous dehydrolysis of silica.

— Stage II (≥500–≤1400°C): breakdown of the local structural order of phenol resin and formation of C domains with graphite-type short-range-order. C coexists with non-crystalline SiO_2 containing low amounts of OH-groups. The C and SiO_2 domains up to ≈ 1000°C are extremely small (≤1 nm). At higher temperatures, C and SiO_2 domains become larger (≈ 2–3 nm at 1400°C) and develop partial ordering of the short-range structure.

1 Introduction

Different routes have been used to produce SiC, starting with metal organic materials. In an early work Prochazka[1] synthesized β-SiC powders by vapor phase decomposition of halogenated silanes. SiC synthesis by laser or plasma driven CVD methods have also been reported.[2,3] The most widely studied SiC synthesis process using metal organic starting materials is pyrolysis of polysilanes and polycarbosilanes.[4–6] Zhang *et al.*[7] mentioned in a recent paper that the thermal decomposition of polymethylsilane to polycarbosilane takes place at 400°C. Above this temperature a hydrogenated non-crystalline SiC-phase is being formed, transforming to β-SiC at about 1000°C with some small amount of coexisting α-SiC. β-SiC powders can also be processed from tetramethoxysilane and phenol resin by H_2O polymerization.[8] The reaction is believed to take place through an intermediate non-crystalline precursor stage consisting of SiO_2 plus C. Reaction of SiO_2 with C to SiC was observed above about 1200°C. The present study provides additional information on the structural development of the latter precursor prior to SiC crystallization. Nuclear magnetic resonance spectroscopy, X-ray diffraction, transmission electron microscopy, and the large-angle X-ray scattering methods have been used to solve the problem.

2 Processing Conditions

SiC precursors were prepared from tetramethoxysilane ($Si(OCH_3)_4$, TMOS Trichemical Co., Japan), and resol-type phenolic resin (phenol formaldehyde condensate, J-325, Dainippon Ink and Chemicals, Inc., Japan). The molar ratio of water to alkoxide in the starting admixture was 1. The TMOS is 6 N pure and yields SiO_2 after polymerization. The phenolic resin has a molecular weight of 600–650 g/mol. It is thermally set to

Table 1. Description of samples used for the investigations

Sample key	*Heat treatment temperature (°C)*[+]	*Characterization techniques*
ST16 (as-received)	≈80[§]	XRD, LAXS, NMR
ST16-3	300	XRD, NMR
ST16-4	400	XRD, LAXS
ST16-6	600	XRD, NMR
ST16-8	800	XRD, LAXS, NMR
ST16-10	1000	XRD, NMR, TEM
ST16-12	1200	XRD, LAXS, TEM
ST16-13	1300	XRD, TEM
ST16-14	1400	XRD, TEM
ST16-17	1750	XRD

[+]Constant heat-treatment duration: 30 min.
[§]As-received sample, dried in a laboratory furnace.
XRD = Standard X-ray diffraction technique.
LAXS = Large-angle X-ray scattering.
NMR = ^{29}Si and ^{13}C nuclear magnetic resonance.
TEM = Transmission electron microscopy.

polymer resin below 80°C and it transforms to an amorphous carbon at temperatures higher than about 500°C. The carbon yield from the phenolic resin is 35·4 wt% after heat-treatment at 1000°C in N_2 atmosphere. TMOS and phenolic resin were mixed with H_2O and ethyl alcohol, with a weight ratio of TMOS and phenol resin of 1:0·76 to form a gel. After forming a gel by polymerization, the admixture was dried at about 80°C in a laboratory furnace. The resulting product (designated as 'as-received material') appears as a dark brown transparent solid.

The as-received material was heat-treated for 30 min in the temperature range between 300 and 1750°C in flowing N_2 gas. A tabulation of investigations carried out with various samples is given in Table 1.

The plot of weight losses versus heat-treatment temperatures shows that there are 3 distinctive stages leading to SiC formation. During the first stage, from the as-received state to about 500°C,

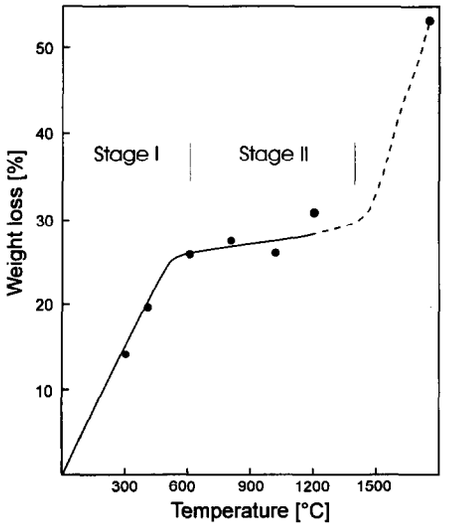

Fig. 1. Weight loss of the as-received SiC precursor material plotted against heat-treatment temperature.

the weight loss increases gradually with temperature. There is no change during the second stage between 500– ≈1400°C. The third stage between 1400 and 1750°C shows again a strong temperature dependency of weight loss (Fig. 1).

3 Experimental Procedure

3.1 X-ray diffractometry (XRD)

Powder XRD studies were carried out at room temperature with a computer–controlled Siemens D5000 powder diffractometer (CuK_α-radiation). The diffractograms were recorded in the 10 to 80° 2θ-range in the step-scan mode (5 s/0·01°, 2θ).

3.2 Large-angle X-ray scattering (LAXS) measurements

The diffuse spectrum scattered by the sample irradiated with graphite-monochromatized molybdenum K_α radiation was obtained by using an automatic diffractometer.[9] 500 intensities corresponding to equidistant s points ($s = 4\pi(\sin\theta/\lambda)$, $\Delta s = 0{\cdot}035363$) were collected in the range $2° < \theta < 65°$ (2θ = diffraction angle). The stability of the X-ray flux and of the sample was checked by frequent repetition of measurements at angles conveniently spread out in the θ range. All measurements were carried out at 22°C.

Scattered intensities were corrected for polarization and absorption effects (namely $I_c(s)$), then normalized by comparison, in the vicinity of high θ angles, with the sum of coherent and incoherent independent intensities. The normalization factor K derived from this data treatment is in good agreement with those determined from Norman's[10] and Krogh-Moe's[11] methods. Atomic scattering factors, $f_i(s)$ for all the atoms, were those proposed by Cromer and Waber.[12] Compton diffusion factors were taken from tables published by Cromer.[13]

Reduced intensities, $I(s)$, were calculated as follows:

$$I(s) = KI_c(s) - \Sigma_i n_i [(f_i(s) + \Delta f'_i)^2 + \Delta f''^2_i + I_{i(inch)}(s)]$$

where K is the normalization constant, $I_c(s)$ is the corrected intensities, n_i is the number of atoms f_i in the chosen unit volume, $f_i(s)$ is the atomic scattering factor, $\Delta f'_i$ and $\Delta f''_i$ are the real and imaginary parts of the anomalous dispersion, and $I_{(inch)}(s)$ is the total incoherent radiation for the atom i.

The radial distribution $D(r)$ is then expressed under the form:

$$D(r) = 4\pi r^2 \rho_o + 2\tau\pi^{-1} \int_i^s si(s)M(s) \sin(rs)\, ds$$

where ρ_o is the average electronic density of the sample and $M(s)$ is a modification function defined by $f^2_{ni}(O)/f^2_{ni}(s)\exp(-s^2/100)$.

All calculations were performed by using our

LASIP program[13] the structure of which is similar to the KURVLR program of Johansson and Sandström.[14]

3.3 Nuclear magnetic resonance (NMR) spectroscopy

MAS NMR measurements were carried out using a Bruker MSL 300 spectrometer operating at 75·4 MHz (^{13}C), and 59·4 MHz (^{29}Si).

^{13}C CP TOSS (CP = Cross polarization, TOSS = Total suppression of spinning sidebands) NMR spectra were acquired with typical cross polarization times of 1 ms and recycle delays of 1 s. About 300 scans were accumulated. The MAS frequency was 3·2 kHz. Additionally, single pulse ^{13}C experiments were carried out for the sample heat treated at 800°C (repetition time: 20 s, number of scans: 1500).

Similar conditions were applied to ^{29}Si measurements. ^{29}Si CP TOSS investigations, and, additionally, a series of single pulse spectra were taken in order to estimate the relative amounts of silica in the different Q^n units. Chemical shifts are referenced to TMS both for ^{13}C and ^{29}Si NMR.

3.4 Transmission electron microscopy (TEM)

TEM was performed with a Philips EM430 analytical microscope (300 kV accelerating voltage, LaB_6 filament). Thin foils were prepared using a tripod polisher and subsequent ion beam milling.

4 Results

4.1 X-ray diffractometry (XRD)

The XRD patterns of the SiC precursors show that up to 1400°C the material is non-crystalline. At 1750°C (ST16-17, Table 1) it consists of β-SiC and a trace of graphite.

Despite being non-crystalline, the XRD diagrams of the SiC precursors below 1400°C exhibit very broad diffraction maxima near 3·95 Å. Another very broad and low intense diffraction maximum appears near 2·08 Å. It gradually becomes more intensive with the increase of the annealing temperature.

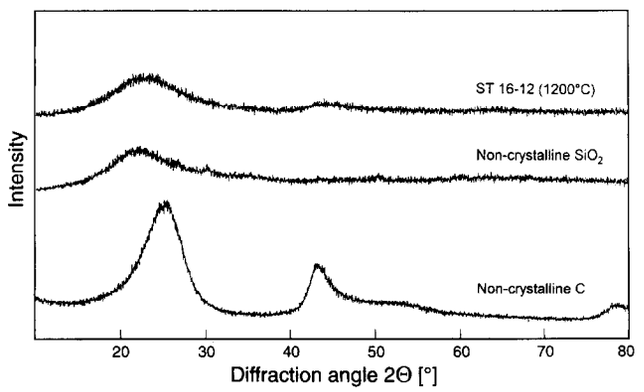

Fig. 2. XRD diagrams of precursor sample ST16-12, heat-treated at 1200°C (Table 1). The XRD patterns of non-crystalline SiO_2 and C are given for comparison.

4.2 Differential radial electron distribution functions (Rdf)

LAXS raw intensity curves of the as-received powder (ST16) and of the sample heat-treated at 1200°C (ST12, Table 1) are drawn in Fig. 3. The LAXS patterns yield strong and broad peaks near 3·95 Å, and weak signals near 2·08 and 1·22 Å. The intensity of the latter peaks increases with temperature. Rdf curves of the as-received and of

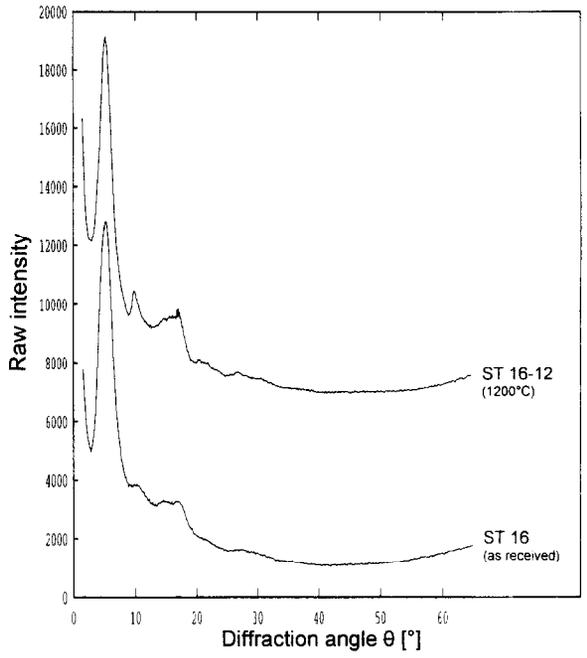

Fig. 3. LAXS raw intensity curves for the as-received sample (ST16) and for the sample heat-treated at 1200°C (ST16-12, Table 1). $Mo_{K\alpha}$ radiation.

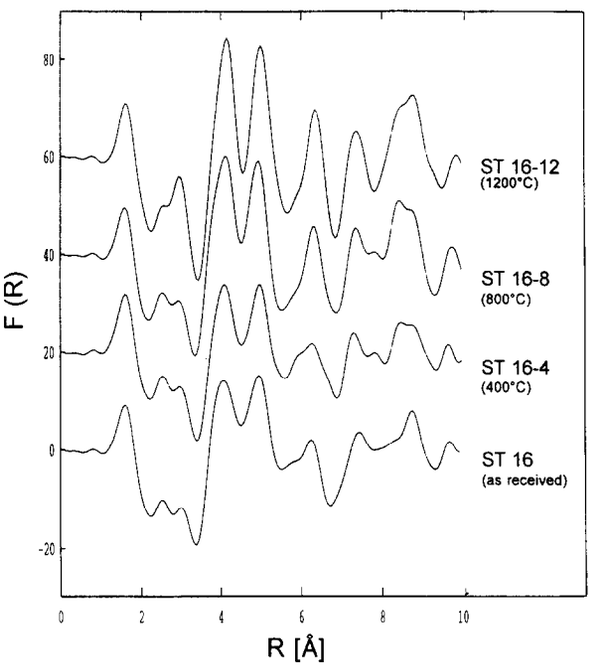

Fig. 4. Differential radial distribution functions (rdf) for the as-received sample (ST16), and for samples heat-treated at 400°C (ST16-4), 800°C (ST16-8), and 1200°C (ST16-12, Table 1).

heat-treated samples show similar features. They can roughly be divided into two domains: below and above R = 5·5 Å (Fig. 4).

- In the first range (R < 5·5 Å), the peaks can readily be assigned to Si–O (1·6 Å), O–O (O_1-Si_1–O_2, 2·6 Å), Si_1–Si_2 (Si_1–O_1–Si_2, 3·3 Å), Si–O_2 (Si_1–O_1–Si_2–O_2, 4·1 Å), and Si_1–Si_3 (Si_1–O_1–Si_2–O_2–Si_3, 5·0 Å). These peak positions lie very close by to those observed for a pure SiO_2 glass.[15-16] The first peak can be taken as internal standard in order to compare the signal intensities, because it always corresponds to the SiO_4 contribution. The peaks at 4·1 Å and 5·0 Å have considerably higher intensities in our samples than in pure SiO_2 glass, except for the samples heat-treated at T ≤ 400°C (samples ST16 and ST16-4, Table 1). This indicates that the short-range-order of the SiO_2 compound is much more regular in our sample as compared to SiO_2. The increase of the intensity of the Si_1–Si_2 peak at 3·3 Å, especially between 800 and 1200°C (samples ST16-8 and ST16-12, Table 1), corresponds to an increase in the size of the partially ordered SiO_2 domains, or to a more narrow distribution of the O–Si–O bonding angles.
- The second range (R > 5·5 Å) in the rdf curves is more difficult to understand, since the peaks cannot be assigned to a specific interaction, but correspond to superpositions of different contributions. However, the main features are also very similar to those observed for pure SiO_2 glass. The samples heat-treated at 800 and 1200°C show an increase of the peak intensities corresponding either to a more regular middle-range-order or to an enlargement of the ordered domains.

4.3 Transmission electron microscopy (TEM)

Bright-field micrographs of samples heat-treated between 1000 and 1400°C appear almost featureless. Dark-field images, however, obtained by a section of the d = 2·08 Å diffraction ring corresponding with non-crystalline carbon (Fig. 5) exhibit remarkable differences between the 1000°C-sample and specimens heat-treated at higher temperature. The latter show domains of few nanometres (Fig. 5), which are assumed to correspond with areas of carbon enrichment. The domain size does not increase significantly from 1200 to 1400°C. No domain-like contrast is detectable in dark field images of samples heat-treated at 1000°C leading to the assumption that carbon clusters, if they exist, are smaller than 1 nm.

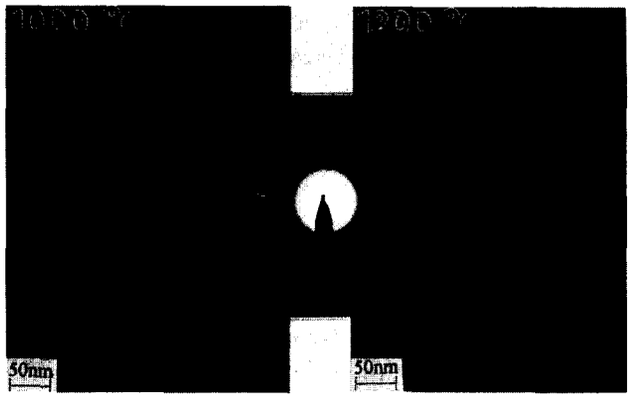

Fig. 5. Dark-field transmission electron micrographs of SiC precursor heat-treated at 1000°C (left) and 1200°C (right) generated by the diffraction ring of d = 2·08 Å (arrow). Bright areas correspond with carbon clusters.

4.4 Nuclear magnetic resonance spectroscopy (NMR)

Figure 6 shows the ^{13}C CP TOSS spectrum. The ^{13}C resonances of the sample ST16 (as-received) and that heat-treated at 300°C (ST16-3, Table 1) can be assigned quite easily using the results of Sojka *et al.*.[17] The signals originate from phenol resin which was used to prepare the samples. Only the low intensity components between 60 and 70 ppm (indicated by stars in Fig. 6) are not yet fully

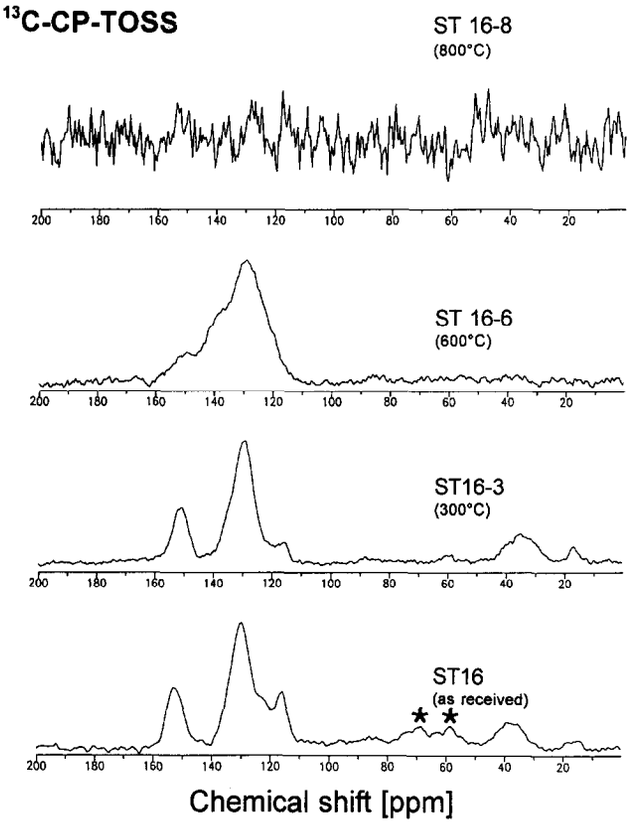

Fig. 6. ^1H–^{13}C CP TOSS NMR spectra (^1H–^{13}C Cross polarization spectra with total suppression of spinning sidebands) of various ST16 samples (Table 1). The spectrum at the bottom corresponds to that of phenol resin (only the two low intensity resonances marked by the stars are not identified as yet, see also text). Phenol resin is decomposed at temperatures above 300°C. At 600°C only sp^2-hybridized C is found. Cross polarization of the sample dried at 800°C gives no signal at all. Hence, there are no CH_x units left.

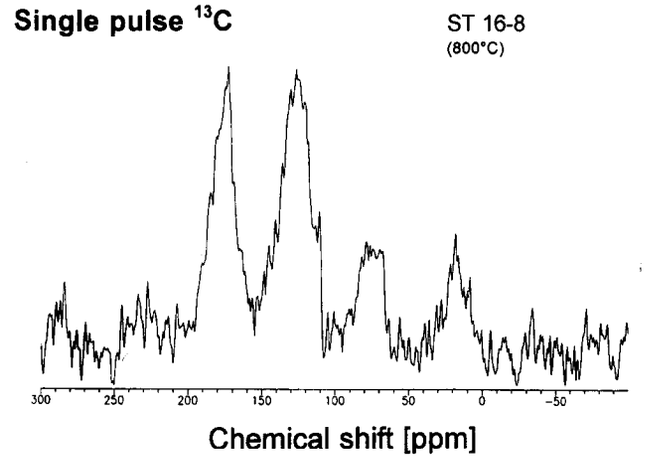

Fig. 7. Single pulse ^{13}C MAS NMR spectrum of sample ST16-8, heat-treated at 800°C (Table 1). The lineshape consists of only one resonance (δ_{iso} = 130 ppm) referring to sp^2-hybridized C with a series of spinning sidebands centered at 180, 75 and 20 ppm.

understood. It is likely that they represent CH_2–O and CH–O units. Heat-treatment of the samples up to 600°C (ST16-6) causes the phenol resin to decompose. A broad resonance at about 130 ppm is found, indicating sp^2-hybridized C. The C is still cross polarized by residual H atoms. However, after heat-treatment of the samples at 800°C (ST16-8) no CP signal is detected, which means that the remaining protons are not associated with C. Single pulse ^{13}C measurements of that sample give only a resonance signal for sp^2-hybridized C with the MAS center band at 120 ppm. The other lines are the spinning side bands equally spaced by the MAS spinning frequency of 4 kHz. They reflect the typical chemical shift anisotropy of about 200 ppm of non-protonated sp^2-hybridized carbon (Fig. 7). There is no hint for sp^3-hybridized carbon.

The situation is different for ^{29}Si NMR. The CP spectra shown in Fig. 8 reveal three different structural units: Q^4 (–112 ppm, SiO_4), Q^3 (–102 ppm, SiO_3OH), and to a minor extent Q^2 groups (–92 ppm, $SiO_2(OH)_2$). In contrast to ^{13}C NMR there is still a CP signal at an annealing temperature of 800°C (ST16-8, Table 1). This indicates that apparently some trace of H atoms is incorporated in the SiO_2 network, forming Q^3 units. The major amount with Q^4 groups, of course, is not cross-polarized. This can clearly be identified by single pulse experiments as shown in Fig. 9 for samples heat-treated at 300 and 800°C. Spectra of single pulse experiments are difficult to deconvolute into three Gaussian lines. But clearly a continuous decrease of the ratios $Q^2:Q^3:Q^4$ is found with increasing temperatures. Estimated ratios are

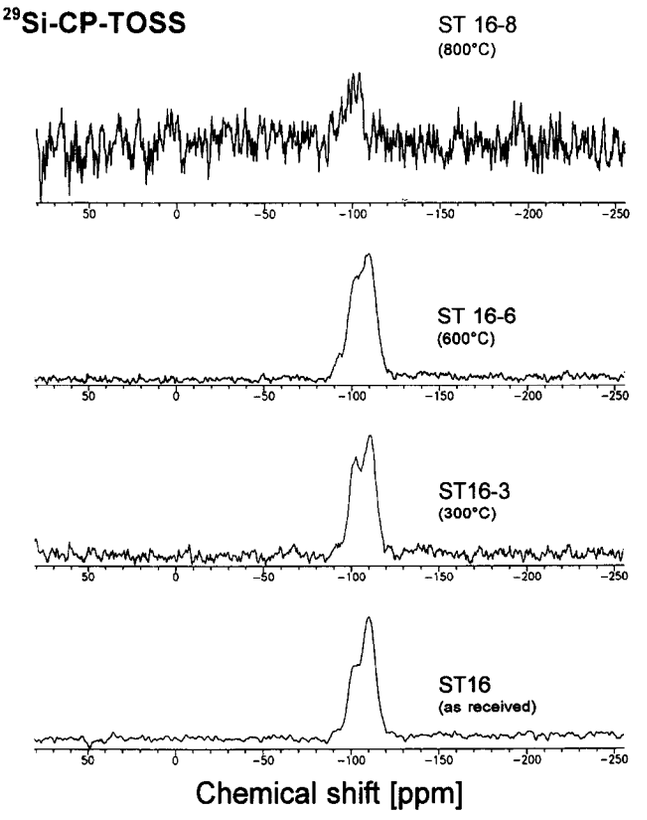

Fig. 8. ^{1}H–^{29}Si CP TOSS NMR spectra (^{1}H–^{29}Si Cross polarization spectra with total suppression of spinning sidebands) of various ST16 samples (Table 1). The spectra for the as-received sample and for the sample heat-treated at 600°C are similar and show Q^4 (SiO_4), Q^3 (SiO_3OH), and a small Q^2 ($SiO_2(OH)_2$) signals (for details see text). At the highest temperature (800°C, ST16-8) only a very weak Q^3 signal is found.

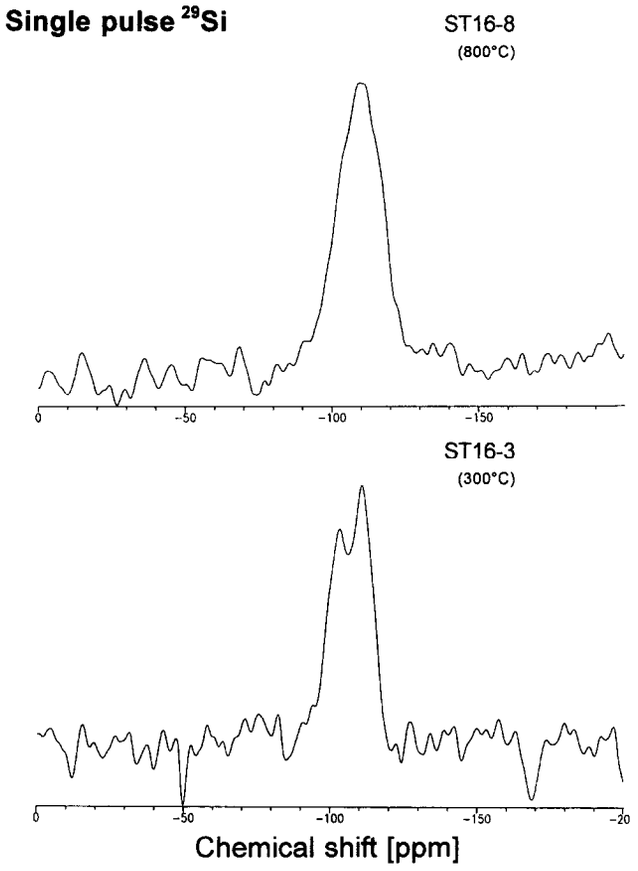

Fig. 9. Single pulse ^{29}Si MAS NMR spectra of the samples ST16-3 and ST16-8 heat-treated at 300 and 800°C, respectively (Table 1). The spectrum at the bottom clearly shows Q^3 (SiO_3OH) and Q^4 (SiO_4) groups in almost equal amounts, whereas only Q^4 units are present after heat-treatment at 800°C.

10:45:45, 5:30:65, and 0:10:90, for the 300, 600, and 800°C samples.

5 Discussion

The Si source material tetramethoxysilane (TMOS) transforms upon hydrolysis and drying at about 80°C to partially hydrogenated SiO_2 (ST16, Table 1). According to the ^{29}Si NMR spectrum, which is very similar to that of dried silica gels,[18] Si occurs as SiO_4 (Q^4), $SiO_3(OH)$ (Q^3) with isolated OH groups, and SiO_2 $(OH)_2$ (Q^2) with two OH groups.[19] There remains the question, whether OH groups are only located in the surface or if they also occur in the bulk of the material. We believe that OH groups are located at the surface and in the volume of the SiO_2 compound.[18] ^{13}C NMR spectra of the sample dried at about 80°C (ST16, Table 1) exhibit peaks which are attributed to phenol resin. Obviously there is no drastic change of the structural short-range-order of the C compound upon hydrolysis and drying the material.

Heat-treatment of hydrolized and dried as-received samples up to 1400°C exhibits 2 different stages in the structural development of the precursors, though all of them are non-crystalline throughout the temperature field investigated (Fig. 2).

Stage I (≤500°C)

Heat-treatment of the as-received material at temperatures to ≤500°C produces strong weight loss (Fig. 1), which is likely due to the gradual decomposition of the phenol resin. This is supported by ^{13}C NMR spectra which gradually and considerably change in this temperature region (Fig. 6). It is especially striking to note that the peaks previously present at about 18 and 35 ppm gradually disappear leaving a rather broad resonance pattern between 120 and 150 ppm in samples heat-treated at 600°C. Rdf curves of the SiC precursor heat-treated at 400°C (ST16-4, Table 1) can also be interpreted in a similar way. Intensities of all rdf peaks, except those at 2·5 and 3·3 Å, become weaker than the peaks of the as-received material (Fig. 4), indicating gradual decomposition of the local structural order in phenol resin.

^{29}Si NMR data (Fig. 8) indicate dehydrolysis of the SiO_x $(OH)_{4-x}$ network to take place. This is evidenced by the deconvolution of the spectra, exhibiting gradual disappearance especially of Q^2 $(SiO_2(OH)_2)$ units.

Stage II (≥500 – ≤1400°C)

Heat-treatment of the SiC precursor in the temperature range of reaction Stage II yields only little weight loss (Fig. 1). ^{29}Si NMR spectra (Figs 8 and 9) and rdf curves (Fig. 4) suggest that non-crystalline SiO_2 is a major compound of the precursors. According to ^{29}Si NMR data (Fig. 8) at 600°C some of the Si bonds are saturated by OH groups distributed throughout the SiO_2 network ('network modifiers'). At 800°C the occurrence of network modifying OH ions becomes less frequent, while at 1200°C the SiO_2 network is OH-ion free. The high intensity of short distance ($R < 5{\cdot}51$ Å) rdf peaks near 4·1 and 5·0 Å suggest that the SiO_2 domains above 400°C have a higher level of structural order than pure fused SiO_2 glasses. The increase of peak intensities in the far distance region ($R > 5{\cdot}5$ Å) of the rdf diagram is interpreted of gradually increasing middle-range-order and of growing sizes of the SiO_2 domains.

^{13}C NMR spectra samples heat-treated at temperatures ≥500°C (Figs 6 and 7) exhibit a complete breakdown of the remaining local structural order of phenol resin and formation of non-crystalline C with sp^2-hybridized graphite-like short-range-order. According to transmission electron microscopic observations the C domains are randomly distributed throughout the SiO_2 matrix (Fig. 5). At 1000°C C domains are below the microscopical resolution (≤1 nm). At 1200°C domain sizes become larger (2–3 nm) though no further increase is observed between 1200 and 1400°C.

Processes taking place at temperatures > 1400°C are beyond the scope of the present study. Referring to weight loss measurements (Fig. 1) and to literature data SiC is formed by reaction of C and SiO_2.[20] The homogeneous mixture of the highly reactive C and SiO_2 compounds yields high SiC formation rates. Ceramics produced from such SiC powders exhibit homogeneous and dense microstructures with favorable fracture toughness, especially in the presence of some finely dispersed graphite particles.[8]

Acknowledgements

H. S. thanks Mr H. Hermanns (Köln) for technical assistance. Dr B. Saruhan (Köln) and S. Schneider (Rheinbach) read the manuscript. This is gratefully acknowledged.

References

1. Prochazka, A., The role of boron and carbon in the sintering of silicon carbide. In *Special Ceramics 6th British Ceramic Research Association*, Stoke on Trent, UK, p. 171, 1975.
2. Kuibira, A., Matsui, A., Hojo, J., & Kato, A., Preparation of SiC and Si_3N_4 powders by RF-plasma. *J. Ceram. Soc. Japan*, **95** (1987) 89.

3. Cannon, W. R., Danforth, S. C., Flint, J. H., Haggerty, J. S. & Mara, R. A., Sinterable ceramic powders from laser driven reactions. I. Process description and modeling. *J. Am. Ceram. Soc.*, (1982) 324–30.
4. West, R., David., L. D., Djurovich, P. I., Yu, H. & Sinclair, R., Polysilastyrene: Phenylmethylsilane – dimethylsilane copolymers as precursors to silicon carbide. *Am. Ceram. Soc. Bull.* **62** (1983) 899–903.
5. Schmidt, W. R., Sukumar, V., Hurley, W. J., Jr. Garcia, R., & Interrante, L. V., Silicon nitride derived from an organometallic polymeric precursor: Preparation and characterization. *J. Am. Ceram. Soc.*, **73** (1990) 2412–8.
6. Wu, H.J. & Interrante, L. V., Preparation of a polymeric precursor to silicon carbide via ring-opening polymerization: synthesis of poly ((methylchlorosilylene)methylene) and poly(silapropylene). *Chem. Mater.*, **1** (1989) 564.
7. Zhang, Z. F., Babonneau, F., Laine, R. M., Mu, Y., Harrod, J. F. & Rahn, J. A., Poly(methylsilane) — A high temperature ceramic yield precursor to silicone carbide. *J. Am. Ceram. Soc.*, **74** (1991) 670–3.
8. Tanaka, H., Kaozhe, J. & Hirota, K., Synthesis and sintering of SiC–C powder mixture from $Si(OCH_3)_4$ and phenol resin. *J. Ceram. Soc. Japan*, **98** (1990) 86–9.
9. Lecante, P., Mosset, A. & Galy, J., LASIP: A liquid and amorphous structure investigation package. *J. Appl. Cryst.*, **18** (1985) 214–8.
10. Norman, N., The fourier transform method for formalizing intensities. *Acta Crystallogr.*, **10** (1957) 370–3.
11. Krogh-Moe, J., A method for converting experimental X-ray intensities to an absolute scale. *Acta Crystallogr.*, **9** (1956) 951–4.
12. Cromer, D. T. & Waber, J. T., Scattering factors computed from relativistic Dirac–Slater wave functions. *Acta Crystallogr.*, **18** (1965) 104–5.
13. Cromer, D. T., Compton scattering factors for aspherical free atoms, *J. Chem. Phys.*, **50** (1969) 4857–60.
14. Johansson, G. & Sandström, M., Computer programs for the analysis of data on X-ray diffraction by liquids. *Chem. Scripta*, **4** (1973) 195–9.
15. Zarzycki, J., *Les Verres et l'Etat Vitreux*, ed. Masson Paris, 1982 p. 83.
16. Himmel, B., Gerber, T. H. & Bürger, H., X-ray-diffraction investigations of silica gel structures. *J. Non-Crystalline Solids*, **91** (1987) 127–36.
17. Sojka, S. A., Wolfe, R. A., Dietz, E. A., Jr. & Dannels, B. F., Carbon-13 nuclear magnetic resonance of phenolic resins. Positional isomers of bis(hydroxybenzyl)phenols and bis-(hydroxyphenyl)methanes. *J. Am. Chem. Soc* **62** (1979) 767–70.
18. Fyfe, C. A., Gobbi, G. C. & Kennedy, G. J. *J. Phys. Chem.*, **89** (1985) 277–81, quoted in: *The physics and chemistry of sol-gel processing*, Sol-Gel Science, Academic Press Inc., San Diego, CA, USA. 1990.
19. Brinker, C. J. & Scherer, G. W., *The physics and chemistry of sol-gel processing*, Sol-Gel Science, Academic Press Inc., San Diego, CA, USA 1990.
20. Tanaka, H. & Kurachi, Y., Synthesis of β-SiC powder from organic precursor and its sinterability. *Ceramics Intern.*, **14**, (1988) 109-15.